Preprint ANL-HEP-CP-04-138, hep-ph/0412146

Theory of W and Z boson production[1]

Pavel M. Nadolsky

High Energy Physics Division, Argonne National Laboratory, Argonne, IL 60439-4815, U.S.A.

Abstract. Success of precision studies in W and Z boson production at the Tevatron and LHC depends on the progress in reducing theoretical uncertainties to the level of $1-2\%$. I review recent developments in theoretical understanding of W and Z boson production and remaining issues to be solved to meet demands of the near-future experiments.

Production of W and Z bosons at $p\bar{p}$ and pp colliders is well-suited for precision tests of hadronic matter and electroweak interactions, due to its relatively simple mechanism and clean experimental signatures. $W^{\pm}$ and Z^0 bosons will be mass-produced in the Tevatron Run-2 and at the Large Hadron Collider (LHC) with the goal to measure electroweak parameters, probe the internal structure of nucleons, and monitor the collider luminosity. Deviations from the predictions of the Standard Model may possibly occur in the W and Z boson data as a result of new gauge interactions, supersymmetry, particle compositeness, or extra spatial dimensions. Searches for new physics are not feasible without adequate evaluation of the large irreducible background of W and Z bosons from the conventional processes.

The measurement of the W boson mass M_W and width Γ_W is an essential component of the Tevatron physics program. In the Standard Model, radiative corrections relate M_W to the square of the top quark mass, m_t^2, and the *logarithm* of the Higgs boson mass, $\log(M_H)$ [1].[2] A high-precision measurement of M_W and m_t constrains the range of M_H allowed within the Standard Model. For example, if M_W and m_t are known within 30 MeV and 2 GeV, respectively, M_H is predicted within 35%. Conversely, comparison of values of M_W, m_t, and M_H measured in different experiments and channels may reveal signs of new physics. The Run-2 plans to measure M_W with accuracy ≈ 30 MeV per channel per experiment, and Γ_W with accuracy 25-30 MeV [2] . The goal of LHC is to reduce δM_W below 10-15 MeV in order to compete with the precision measurement of M_W at the future Linear Collider [3].

At collider luminosities above 1 fb^{-1}, theoretical uncertainties (currently several percent of the cross section) become the dominant source of error in W and Z observables. These uncertainties must be reduced in order to measure the total cross sections with accuracy $< 2\%$ and M_W with accuracy $< 0.04\%$, as envisioned by the Tevatron and LHC programs. Several dynamical factors contribute at the percent level, including QCD ra-

[1] Contribution to the proceedings of the 15th Topical Conference on Hadron Collider Physics (HCP 2004, June 14-18, 2004, East Lansing, MI)

[2] M_W also receives small corrections proportional to M_H^2.

diative corrections of order $\mathcal{O}(\alpha_s^2)$, electroweak corrections of order $\mathcal{O}(\alpha)$, uncertainties in parton distributions, and power corrections to resummed differential cross sections. Tangible progress has been made in exploring these complex factors, mostly by considering each component separately from the rest in order to simplify the problem. Correlations between effects of different dynamical origins have been often neglected, despite their probable significance in the full result. The percent-level QCD and electroweak contributions will have to be integrated into a future framework that would account for their correlations and be practical enough to serve multifaceted purposes of W and Z physics. In this talk, I review the recent advancements and future steps towards development of such a comprehensive model.

Overview of the process. At hadron colliders, the massive electroweak bosons are produced predominantly via $q\bar{q}$ annihilation and detected by the decay into a pair of leptons. A typical W or Z observable is affected by the QCD and electroweak radiation from the hadronic initial state; production, propagation, and decay of massive bosons; and electroweak radiation from the leptonic final state. A hadronic cross section is evaluated in perturbative QCD as a product of hard scattering cross sections and nonperturbative parton distribution functions (PDF's). The hard scattering cross sections are known at $\mathcal{O}(\alpha_s^2)$ for inclusive observables (depending on one energy scale), and at $\mathcal{O}(\alpha_s)$ for observables depending on several energy scales. Phenomenological parametrizations of the PDF's can be taken from a global fit to hadronic data. Uncertainties in the PDF's arising from diverse experimental and theoretical sources can be propagated from the global analysis into the predictions for the W and Z cross sections [4]. When the soft QCD radiation is enhanced in the scattering (*e.g.*, when the transverse momentum q_T of the electroweak boson is much smaller than its invariant mass Q), the finite-order perturbation theory has to be replaced by resummation of large logarithmic corrections through all orders of α_s. The resummation is achieved by modifying the form of QCD factorization in the affected regions in order to absorb the problematic soft logarithms into exponential Sudakov form factors.

The full $\mathcal{O}(\alpha)$ electroweak corrections are known both for W boson production [5] and Z boson production [6]. They depend on the flavor of produced leptons. Not all $\mathcal{O}(\alpha)$ corrections are of equal importance throughout all phase space. The resonant production of W bosons at $Q \approx M_W$ is described well within "the pole approximation" [7], which neglects the subleading WZ box diagrams. For its part, the pole approximation is dominated by virtual corrections to boson propagators and vertices, as well as by QED radiation off the final-state charged leptons [8]. The QED radiation from the initial-state quarks and interference between the initial and final states are of a smaller magnitude numerically, but may have some impact on precision measurements. Away from the W boson resonance ($Q \gg M_W$), the pole approximation becomes unreliable and has to be replaced by the full $\mathcal{O}(\alpha)$ result [9]. Yet higher-order electroweak corrections may be non-negligible as well, especially if enhanced by large logarithms near the boundaries of available phase space or at large boson virtualities. W and Z boson production with radiation of two additional photons has been studied in Ref. [10]. Leading contributions from radiation of multiple soft photons can be resummed through all orders of α, as it was done recently for W decays in Refs. [11, 12].

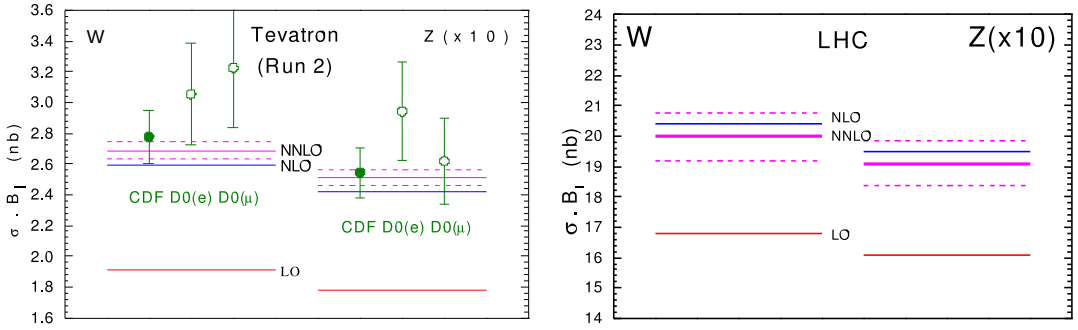

Figure 1. Effect of the $\mathcal{O}(\alpha_s^2)$ (NNLO) corrections on the total cross sections $\sigma_{tot}(p\bar{p}^{(-)} \to (W \to \ell\nu)X)$ and $\sigma_{tot}(p\bar{p}^{(-)} \to (Z \to \ell\bar{\ell})X)$ at the Tevatron and LHC [13]. The narrow-width EW approximation was used.

Total cross sections. The interplay of various factors can be most easily demonstrated on the example of the total cross sections, given in perturbative QCD by

$$\begin{aligned}\sigma_{tot}(p\bar{p}^{(-)} \to (V \to \ell_1\ell_2)X) &= \sum_{a,b=q,\bar{q},g} \int dx_1 dx_2\, f_{a/p}(x_1,\mu)\, f_{b/\bar{p}^{(-)}}(x_2,\mu) \\ &\times \ \widehat{\sigma}_{tot}(ab \to (V \to \ell_1\ell_2)X). \end{aligned} \tag{1}$$

Here $V = W$ or Z; $\ell_1\ell_2$ are the charged lepton and neutrino ($\ell\nu$) in W boson production, or the charged lepton and antilepton ($\ell\bar{\ell}$) in Z boson production; $\widehat{\sigma}_{tot}$ are the hard scattering cross sections, known to $\mathcal{O}(\alpha_s^2)$ [14, 15]; and $f_{a/p}(x,\mu)$ are the parton distributions. The integration is over the partonic momentum fractions x_1 and x_2, and the summation is over the relevant parton flavors. The W and Z total cross sections have been evaluated recently by the MRST group by using the parton distributions from a recent global analysis, realized with inclusion of all known next-to-next-to-leading-order, or NNLO, corrections [13]. The $\mathcal{O}(\alpha_s^2)$ correction was found to increase σ_{tot} by about 4% at the Tevatron and reduce σ_{tot} by about 2% at the LHC [cf. Fig. 1]. The dependence of σ_{tot} on the arbitrary factorization scale μ is reduced at $\mathcal{O}(\alpha_s^2)$ to about 1%, suggesting high stability with respect to QCD corrections of order α_s^3 and beyond.

The magnitude of $\mathcal{O}(\alpha)$ electroweak corrections is comparable to that of the QCD corrections. In the limit of the vanishing boson's width Γ_V, the production of the vector bosons can be separated from their decay, by introducing on-shell production cross sections $\sigma_{tot}(p\bar{p}^{(-)} \to V)$ and branching ratios $\mathrm{Br}(V \to \ell_1\ell_2)$:

$$\sigma_{tot}(p\bar{p}^{(-)} \to (V \to \ell_1\ell_2)X) = \sigma_{tot}(p\bar{p}^{(-)} \to V) \cdot \mathrm{Br}(V \to \ell_1\ell_2). \tag{2}$$

At this level of accuracy, the branching ratio defined via Eq. (2) coincides with the partial width, $\mathrm{Br}(V \to \ell_1\ell_2) = \Gamma(V \to \ell_1\ell_2)/\Gamma_V$. The partial width can be defined beyond the Born level as a universal pseudo-observable, included in concrete cross sections via process-specific relations. For instance, the partial widths for Z bosons are incorporated in the fit to the LEP Z-pole observables with the help of a complicated procedure, which accounts for the Z line shape, initial- and final-state electroweak radiation, and γZ

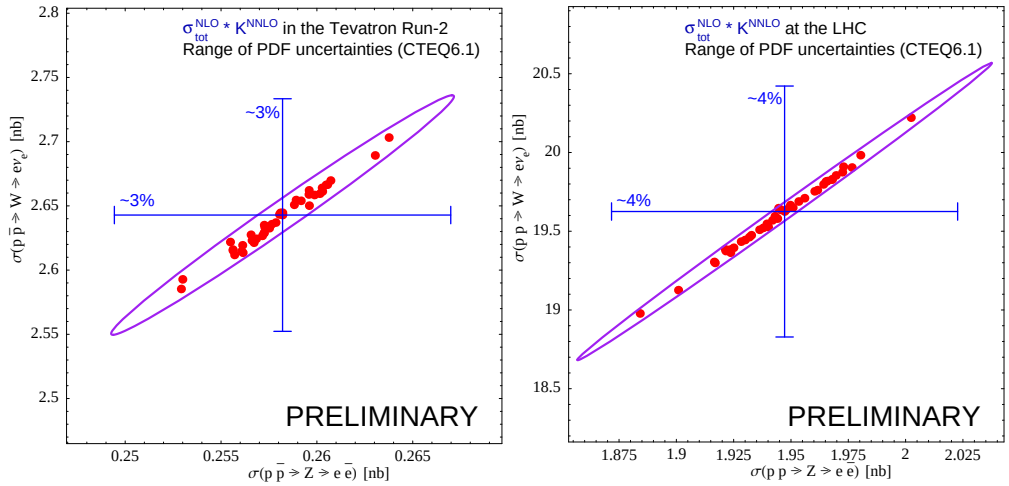

Figure 2. Correlations between the total W and Z cross sections at the Tevatron and LHC found in the new CTEQ analysis [17]. The cross sections are computed at $\mathcal{O}(\alpha_s)$ and rescaled by the NNLO K-factor, extracted from Ref. [13]. The dots correspond to 41 PDF sets from the CTEQ6.1 analysis [18].

interference (see "The Z boson" review in Ref. [16]). An analogous (but not identical) procedure relates the partial widths to the Tevatron cross sections. A tree-level estimate in the Standard Model yields $\Gamma(W \to \ell\nu)/\Gamma_W = 11\%$ and $\Gamma(Z \to \ell\bar{\ell})/\Gamma_Z = 3.3\%$, while the Review of Particle Physics quotes $(10.68 \pm 0.12)\%$ and $(3.3658 \pm 0.0023)\%$ based on the fit to the world (predominantly LEP) data [16]. The shown RPP values are averaged over three lepton generations. Consequently the narrow-width approximation may deviate from the true Tevatron cross sections by up to $\sim 3\%$, if the Tevatron-specific $\mathcal{O}(\alpha)$ corrections are not taken into account.

In addition, the narrow-width approximation neglects the Breit-Wigner line shape of vector bosons and is not suitable for computation of differential distributions. The next level of refinement is realized in the effective Born approximation (EBA), which includes the final width and radiative corrections to the electroweak couplings and boson's propagator (but no effects of real particle radiation). With (without) lepton identification requirements, the EBA W cross section in Run-2 exceeds the full $\mathcal{O}(\alpha)$ cross section by 2% (4%) in the $e\nu_e$ decay channel, and 6% (2%) in the $\mu\nu_\mu$ decay channel [9]. As can be seen from this discussion, the electroweak corrections may induce sizable variations in σ_{tot}. A percent-level comparison of the total cross sections is only meaningful if the employed electroweak corrections are well-documented and consistent.

Uncertainty in σ_{tot} due to imprecise knowledge of parton distributions can be evaluated using one of the available methods [4]. The exact values of the PDF errors depend on the conventions adapted by each group, but all lie in a few-percent range. The CTEQ estimate (based on the most conservative criterion among all groups) quotes the PDF error of 3% (4%) at the Tevatron (LHC). The PDF errors for W and Z total cross sections are highly correlated [cf. Fig. 1], reflecting the striking similarity between the quark-dominated initial states of the two processes. The ratio of the two cross sections, $R_{W/Z} = \sigma_{tot}(W)/\sigma_{tot}(Z)$, is essentially invariant with respect to the changes in the par-

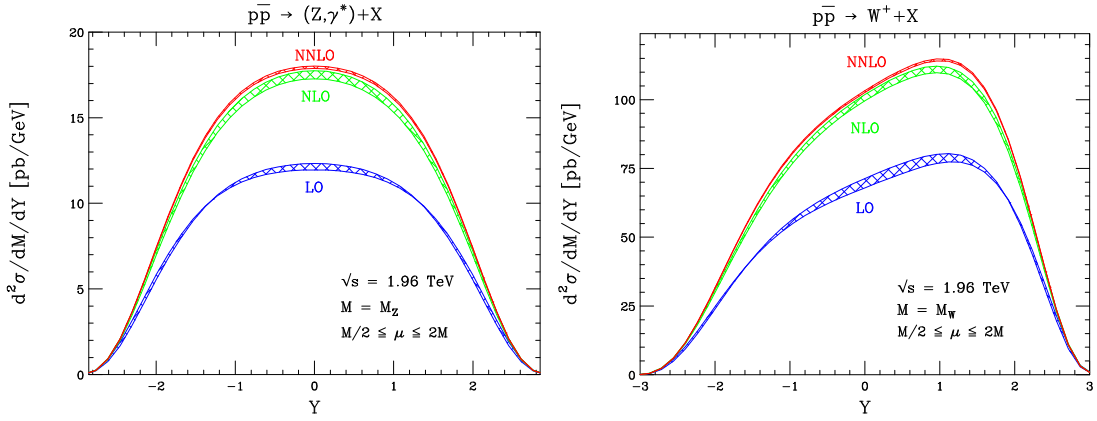

Figure 3. $\mathcal{O}(\alpha_s^2)$ rapidity distributions in the Tevatron Run-2 [21].

ton distributions. A measurement of Z boson cross section can tightly constrain the PDF input in W boson production and other kindred processes. Furthermore, fluctuations in the Z boson rate in the course of the collider run would reflect changes in the collider luminosity, which can be controlled through the measurement of $\sigma_{tot}(Z)$ to the level of $1-2\%$. These nice features of the W and Z boson total cross sections advance them as likely "standard candle" monitors of the partonic and collider luminosities at the LHC [19]. Of course, all percent-level effects must be put together in one calculation to realize this goal. To reconstruct the total cross section from the visible events, an accurate model of the detector acceptance is needed. The W boson acceptances can be controlled at the level of 2% by incorporating the parton-level NLO cross sections into parton showering programs [20].

Rapidity distributions of massive electroweak bosons have been recently computed at $\mathcal{O}(\alpha_s^2)$ with the help of a novel technique based on the optical theorem and recursive reduction of arbitrary loop integrals to a small set of known "master integrals" [21]. In a large range of rapidities ($|y| < 2$), the $\mathcal{O}(\alpha_s^2)$ correction leads to essentially uniform enhancement of the cross section by $3-5\%$ in Z production and $2.5-4\%$ in W production [cf. Fig. 3]. The $\mathcal{O}(\alpha_s^2)$ corrections are augmented and less uniform in the forward rapidity regions. Similarly to the total cross sections, the scale dependence is reduced in $\mathcal{O}(\alpha_s^2)$ rapidity distributions below 1%.

The shape of the rapidity distributions is determined by the x dependence of parton densities. W boson production is sensitive to the flavor composition of the PDF's because of the mixing of quark flavors in $Wq\bar{q}$ coupling. At the $p\bar{p}$ collider Tevatron, W bosons predominantly probe the distributions of u and d quarks (recall that the distribution of d antiquarks in an antiproton is equal to the distribution of d quarks in a proton). The CTEQ and MRST analyses include the Tevatron W cross sections in the form of the charge asymmetry

$$A_{ch}(y_\ell) \equiv \frac{d\sigma^{W^+}/dy_\ell - d\sigma^{W^-}/dy_\ell}{d\sigma^{W^+}/dy_\ell + d\sigma^{W^-}/dy_\ell},$$

defined in terms of the rapidity distributions $d\sigma^{W^\pm}/dy_\ell$ of high-p_T charged leptons from $W^\pm$ boson decays [22]. At forward y_ℓ, the Tevatron charge asymmetry probes the ratio

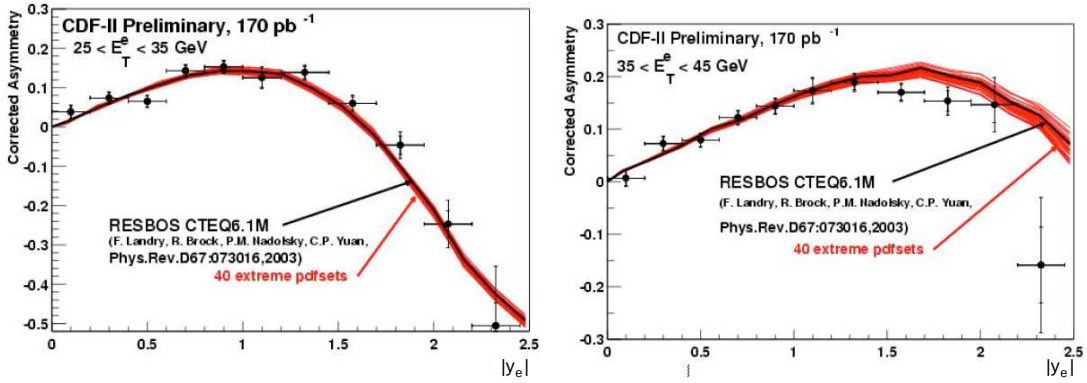

Figure 4. The CDF Run-2 charge asymmetry vs. the resummed result from the q_T resummation program RESBOS [23, 24]. The bands reflect the PDF uncertainty, evaluated using the CTEQ6.1 PDF set [18].

$d(x,M_W)/u(x,M_W)$ at x up to about 0.3. In the experiment, selection cuts are imposed on the transverse energies E_T of the charged leptons and neutrinos as a means to suppress the backgrounds and discriminate between different ranges of x. The preliminary CDF Run-2 asymmetry is in a good agreement with the resummed theory cross section at $25 < E_T^e < 35$ GeV [Fig. 4(a)], but some points fall out of the CTEQ PDF uncertainty band at $35 < E_T^e < 45$ GeV [Fig. 4(b)], indicating the need in further improvements of the PDF model.

If the transverse momentum q_T of W boson is neglected, a simple kinematic relationship exists between the rapidity y_ℓ and transverse momentum $p_{T\ell}$ of the charged lepton. This relationship induces a strong correlation between the shapes of $A_{ch}(y_\ell)$ and $d\sigma/dp_{T\ell}$, so that a measurement of $A_{ch}(y_\ell)$ reduces the PDF uncertainty in $d\sigma/dp_{T\ell}$ and the measured W boson mass [25]. While being a helpful approximation, this correlation does not hold exactly, due to non-zero q_T of W bosons and acceptance constraints on the leptonic momenta. If no acceptance cuts are imposed, the charge asymmetry is essentially invariant with respect to the QCD corrections [Fig. 5(a)]. The acceptance cuts re-introduce the sensitivity of $A_{ch}(y_\ell)$ to QCD corrections, due to the differences in phase space available at different orders of perturbative calculation. In Fig. 5(b), differences can be noticed between the leading-order, next-to-leading-order, and resummed cross sections, caused by different shapes of q_T distributions in the three calculations. The differences are augmented at forward rapidities, where the convergence of perturbation series is reduced by enhancement of near-threshold radiation. These features suggest that the $\mathcal{O}(\alpha_s^2)$ corrections cannot be replaced by a constant K-factor at forward rapidities. An additional study may be needed to evaluate the impact of QCD radiation and phase space restrictions on the observed $A_{ch}(y_\ell)$.

p_T distributions and extraction of M_W. The line shape of W bosons is not observed in the leptonic channels because of the missing information about the longitudinal momentum of the neutrino. For this reason, the W boson mass is commonly deduced from the distribution of the transverse momenta of the decay leptons. The distribution in the leptonic transverse mass, $M_T^{\ell\nu} \equiv \sqrt{(|\vec{p}_{T\ell}|+|\vec{p}_{T\nu}|)^2-(\vec{p}_{T\ell}+\vec{p}_{T\nu})^2}$, was the preferred observable to extract M_W in Run-1 because of its reduced sensitivity to the mechanism

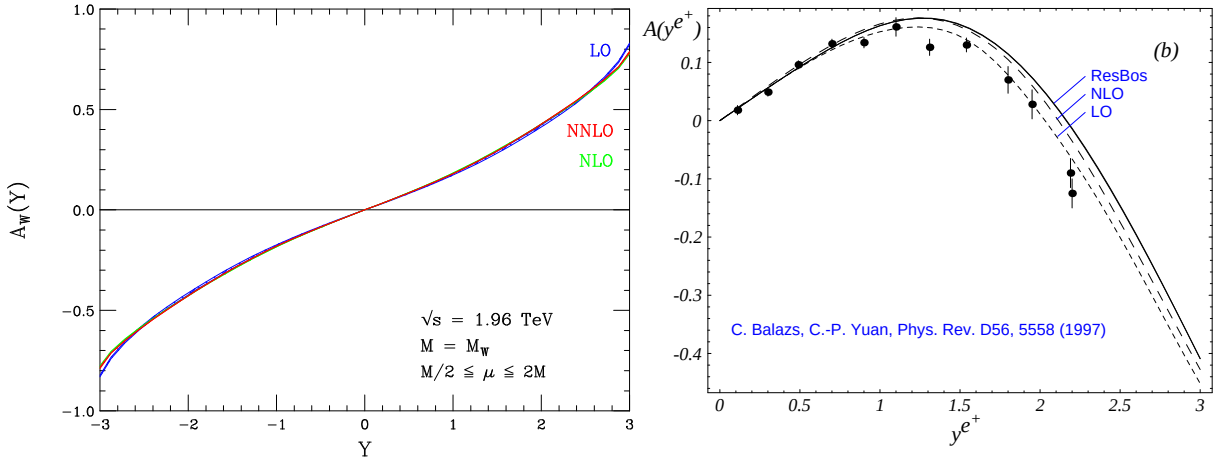

Figure 5. (a) Charge asymmetry $A_{ch}(y)$ of W boson rapidity distributions, $d\sigma/dy$, at various orders of α_s (no acceptance cuts are imposed) [21]; charge asymmetry $A_{ch}(y_\ell)$ in the Tevatron Run-1 for $q_T < 30$ GeV, $p_T^{e^+,\nu} > 25$ GeV in the leading-order, next-to-leading order, and resummed calculations [23].

of W boson production. The kinematical (Jacobian) peak in the $M_T^{\ell\nu}$ distribution is located exactly at $M_T^{\ell\nu} = M_W$ at the Born level and smeared by the W boson's width and radiative corrections. The shape of the Jacobian peak is not affected, to the first order, by the transverse motion of W bosons, caused predominantly by their recoil against the soft QCD radiation. For this reason, extraction of M_W from a fit to the $M_T^{\ell\nu}$ distribution is less reliant on precise knowledge of the q_T spectrum of W bosons and PDF's, which is crucial in the other methods [26]. However, the accuracy of the $M_T^{\ell\nu}$ method suffers from the limited precision in the measurement of the neutrino's transverse momentum (equated in the experiment to the missing transverse energy, $\not\!\!E_T$). An alternative technique extracts M_W from the transverse momentum distribution of the charged lepton, $d\sigma/dp_{T\ell}$. This method does not suffer from the complications associated with the reconstruction of $\not\!\!E_T$, but, as a trade-off, it requires to precisely know the q_T distribution. The direct measurement of $d\sigma/dq_T$ involves reconstruction of $\not\!\!E_T$ and has low precision. A better prediction for the q_T spectrum can be made within the theoretical model by applying the resummation methods described below. The W boson mass can be also extracted from the p_T distribution of the neutrinos, or the ratios $[d\sigma/M_T^{\ell\nu}(W)]/[d\sigma/M_T^{\ell\bar{\ell}}(Z)]$ and $\sigma_{tot}(W)/\sigma_{tot}(Z)$ of W and Z transverse mass distributions and total cross sections [2, 27, 28, 29]. The systematical error tends to be smaller in the last two methods because of the cancellation of common uncertainties in the ratio of W and Z cross sections. However, the reduced systematical uncertainty is balanced in the full result by a larger statistical error, propagated into M_W from a smaller cross section for Z boson production. The uncertainties on M_W will be comparable in all methods towards the end of Run-2, and several techniques will be probably employed by the experimental collaborations as a way to cross check the systematics.

Factorization at small transverse momenta. The reliability of the finite-order cross section is jeopardized at small q_T by incomplete cancellation of soft QCD singularities, which leaves large logarithms $\ln^n(q_T/Q)$ in the hard matrix elements. A re-arrangement

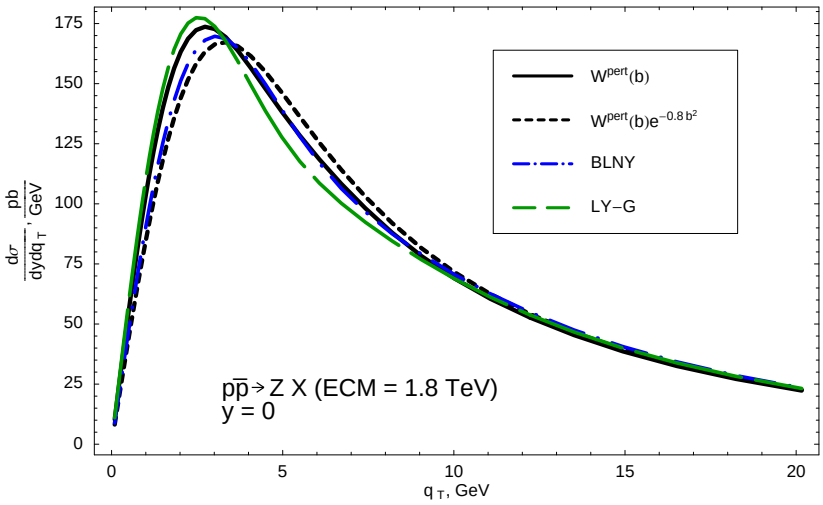

Figure 6. The CSS resummed cross sections in Z boson production at the Tevatron. The curves are computed in several models for the CSS form factor $W(b)$ at large impact parameters ($b > 1$ GeV^{-1}): (a) $W(b)$ at large b is given by extrapolation of its perturbative part from $b < 1$ GeV^{-1} (solid); (b) the same as (a), multiplied by a Gaussian smearing term $e^{-0.8b^2}$ (short-dashed); (c) a phenomenological BLNY form, which shows good agreement with the Run-1 Z data (dot-dashed) [24]; (d) an updated Ladinsky-Yuan form, which shows worse agreement with the Run-1 Z data (long-dashed) [24]. Note that the extrapolation model (curves (a) and (b)) must include a Gaussian smearing term e^{-gb^2}, with $g \sim 0.8$ GeV^2, in order to be close to the BLNY form (and, hence, to the data).

of the perturbation series cures the instability of the theory at $q_T^2 \ll Q^2$ by summing the troublesome q_T logarithms through all orders of α_s into a soft (Sudakov) form factor [30]. The validity of such re-arrangement is proved by a factorization theorem in the method by Collins, Soper, and Sterman (CSS) [31]. The resummation in vector boson production is a special case of a more general problem, and essentially the same method applies to hadroproduction in e^+e^- scattering [32], and semi-inclusive hadroproduction in deep-inelastic scattering [33, 34, 35]. The CSS formalism automatically preserves the fundamental symmetries (renormalization- and gauge-group invariance, energy-momentum conservation) and is convenient in practice. The q_T resummation can be extended to include effects of particle thresholds [36], heavy quark masses [37], and hadronic spin [38, 39]. RESBOS [23, 24] is a Monte-Carlo integrator program that quickly and accurately evaluates the CSS resummed cross sections in Drell-Yan-like processes.

All small-q_T logarithms arise in the CSS method from the form factor $W(b)$ in impact parameter (b) space, composed of the Sudakov exponential and b-dependent parton distribution functions. The resummed q_T distribution is obtained by taking the Fourier-Bessel transform of $W(b)$ into q_T space (realized numerically in RESBOS). The alternative approaches evaluate the Fourier-Bessel transform of the leading logarithmic towers analytically, with the goal to improve transition from the resummed cross section to the finite-order cross section at intermediate q_T [40, 41]. The integration over all b in the Fourier-Bessel transform introduces sensitivity to the nonperturbative QCD dynamics

at $b > 1$ GeV^{-1}. In W and Z boson production, the nonperturbative terms are strongly suppressed by the shape of $W(b)$, as well as by the oscillations in the Fourier-Bessel transform integrand at large q_T. Nonetheless, mild sensitivity to the large-b behavior remains at $q_T < 10$ GeV, contributing on the top of the overall shape that is tightly constrained by the perturbative contributions. The position of the peak in $d\sigma/dq_T$ can move by several hundred MeV depending on the choice of the nonperturbative model [cf. Fig. 6]. The range of uncertainty in the W boson's q_T distribution is substantially reduced by requiring the nonperturbative model to agree with the measured q_T distribution in Z boson production. In Run-1, the uncertainty in M_W due to incomplete knowledge of the $q_T$spectrum of W bosons was estimated to amount to 15-20 MeV.

While significant effort has been put into the study of $W(b)$ at large b [36, 42, 43, 44], none of the existing approaches was able so far to adequately describe the observed Z boson distribution without introducing free parameters.[3] However, a fit of good quality can be made to both Z boson and low-energy Drell-Yan data once a small number of free parameters is allowed in the fit to describe the unknown power corrections [24]. Variations of these parameters lead to small changes in the q_T spectrum of Z bosons and large changes in the low-Q Drell-Yan distributions. The Z boson data taken alone also does not constrain the dependence of the nonperturbative terms on Q and parton flavor. Consequently a combination of Drell-Yan and Z boson data imposes tighter constraints on the nonperturbative parameters than the Z boson data by itself, pretty much as a combination of the inclusive data from various experiments places better constraints on the PDF's than each individual experiment.

The feasibility of such a global p_T fit crucially relies on the universality of the nonperturbative contributions. Whether the universality holds is a question under active investigation. Universality of the large-b contributions follows from the factorization theorem for the resummed cross sections, which was stated in [31] and recently proved in [45]; see also the related discussion in Ref. [44]. A high-quality fit to p_T data from diverse experiments would provide, in principle, empirical confirmation of the universality. The fits utilizing the b_* anzatz [31] – the simplest model of the nonperturbative terms – can indeed achieve a decent χ^2 of 170 (130) per 120 data points for the parameter b_{max} equal to 0.5 (0.8) GeV^{-1}. However, the issue needs further investigation because of the substantial uncertainties in the interpretation of the fits, mostly associated with the low-energy Drell-Yan data. The preferred form of the nonperturbative function is strongly correlated with the overall normalizations of the Drell-Yan cross sections, which, in their turn, are affected by $\mathcal{O}(\alpha_s^2)$ corrections (of order $10-15\%$ [46]), the PDF's, and experimental uncertainties. The true uncertainty in the nonperturbative function is linked to the rest of the factors, which are not under sufficient control yet in the Drell-Yan process. This is particularly true with respect to the PDF parameters, which in principle should be fitted together with the nonperturbative function to obviate correlations between the shape of $d\sigma/dq_T$ and parton densities.

---

[3] It is worth pointing out that the global features of W and Z q_T distributions are uniquely determined by the perturbative contributions and agree well in the different approaches. The challenging part is to describe mild variations at q_T below 10 GeV, which cannot be neglected in high-precision measurements.

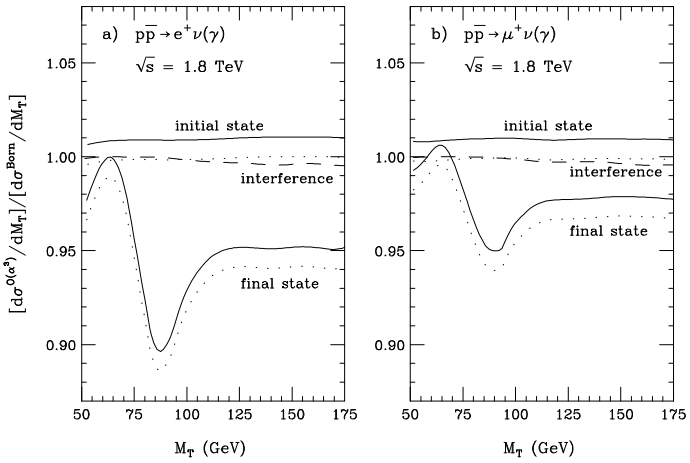

Figure 7. The $\mathcal{O}(\alpha)$ electroweak corrections to the leptonic transverse mass distribution, $d\sigma/dM_T^{\ell\nu}$, in W boson production [7]. No leptonic detection constraints are imposed.

Electroweak corrections to M_W are dominated by the QED radiation from the final-state charged lepton, which results in some loss of the charged lepton's momentum to the surrounding cloud of soft and collinear photons. The final-state QED (FQED) radiation changes the extracted value of M_W by shifting the Jacobian peak in the $M_T^{\ell\nu}$ distribution in the negative direction [cf. Fig. 7]. In contrast, the initial-state radiation and interference terms mostly change the overall normalization of the Jacobian peak and have a smaller effect on M_W. The size of the electroweak corrections depends on the mode of lepton identification. The collinear photons are merged with the electrons in the calorimeter towers, but isolated from the muons in the muon detectors. Consequently the corrections in the electron channel are larger than in the muon channel in the absence of lepton identification requirements, but smaller once the lepton identification is taken into the account. The CDF Run-1b analysis estimates the shift in the W boson mass due to the FQED radiation by -65 ± 20 MeV and -168 ± 10 MeV in the $e\nu$ and $\mu\nu$ decay channels, respectively [47]. The errors of 20 and 10 MeV correspond to the radiative corrections that were ignored in the Run-1 analysis, such as the $\mathcal{O}(\alpha)$ initial-state radiation and interference, or radiation of two and more photons. These errors need to be reduced to push the total δM_W down to 30 MeV in the Run-2 measurement.

The correlations between q_T **spectrum, partonic structure, and electroweak radiation** may prove to be consequential for the upcoming analyses, given that all three are the major sources of uncertainties in the extracted W boson mass. In Run-1, these interconnections were mostly discarded, so that, for instance, simulations of the QCD radiation and electroweak radiation were performed by independent computer programs (RESBOS [23, 24] and W/ZGRAD [6, 7]) and combined *ad hoc* in the final output.

Starting from the Run-2, the correlations between the dominant factors cannot be dismissed. The FQED radiation contributes the bulk of the full electroweak correction, and it cross-talks with the initial-state QCD radiation through conservation of momentum and spin. The combined effect of the $\mathcal{O}(\alpha)$ FQED correction and the resummed QCD correction was estimated for the Run-2 observables by using a new computer program RESBOS-A (RESBOS with FQED effects) [48]. The FQED and resummed QCD cor-

rections to the Born-level shape of the Jacobian peak in the $M_T^{\ell\nu}$ distribution were found to be approximately (but not completely) independent. The reason is that the $M_T^{\ell\nu}$ distribution is almost invariant with respect to the transverse momentum of W bosons, so that the QCD correction reduces, to the first approximation, to rescaling of the Born-level $M_T^{\ell\nu}$ distribution by a constant factor. The relationship between FQED and QCD corrections is more involved in the leptonic p_T distributions, which depend linearly on q_T of W bosons. In the $p_{T\ell}$ channel, the combined effect does not factorize into separate FQED and QCD corrections to the Born-level cross section. Additional modifications will be caused by the FQED correction to the finite part of the resummed cross section (Y-piece) and finite resolution of the detector, which were not considered in Ref. [48].

The PDF uncertainties were estimated in Run-1 by repeating the analysis for select sets of parton densities, which did not cover the full span of allowed variations in the PDF parameters. A more systematical estimate can be realized by applying the new techniques for the PDF error analysis. The choice of the PDF set affects $q_T$distributions directly, by changing the PDF's in the factorized cross section, but also indirectly, by modifying the nonperturbative Sudakov function $S_{NP}(b)$ in the resummed form factor. For a chosen form of $S_{NP}(b)$, the PDF errors can be evaluated within the Hessian matrix method, by repeating the computation of q_T distributions for an ensemble of sample PDF sets. The variations in the resummed q_T spectrum for 41 CTEQ6 PDF sets [49] and BLNY nonperturbative Sudakov function [24] are shown in Fig. 8. Depending on the choice of the PDF set, $d\sigma/dq_T$ changes by up to $\pm 3\%$ from its value for the central PDF set (CTEQ6M). The variations in the PDF's modify *both* the normalization and shape of $d\sigma/dq_T$. Although the changes in the shape are relatively weak at $q_T < 10$ GeV, they cannot be ignored when M_W is extracted from the $p_{T\ell}$ distribution. These results do not reflect possible correlations between the PDF's and $S_{NP}(b)$ in the global fit to p_T data, which may be introduced by the dependence of $S_{NP}(b)$ on the normalizations of the low-Q Drell-Yan cross sections. In contrast to the PDF's, $S_{NP}(b)$ does appreciably modify the shape of $d\sigma/dq_T$ and may cause larger shifts in the extracted M_W. As discussed earlier, the correlation between free parameters in the PDF's and $S_{NP}(b)$ could be explored by performing a simultaneous global analysis of the inclusive cross sections and p_T-dependent data. The first steps towards realization of such a combined fit are being taken within the CTEQ collaboration [17].

The theoretical assumptions need further scrutiny as well, to guarantee their up-to-date level and explore their validity in the new phase space regions accessible in the Run-2 and at the LHC. For example, substantial deviations from the present model may occur in the resummed cross sections at momentum fractions x of order 10^{-2} or less, typical for forward rapidities in the Run-2, and for all rapidities at the LHC [50]. Such deviations may be caused by enhancement of $\ln(1/x)$ terms in the perturbative or nonperturbative parts of the resummed form factor, which could lead to the broadening of q_T distributions at small x. An estimate based on the analysis of small-x semi-inclusive hadroproduction at HERA suggests that the q_T broadening may be visible in a sample of forward-rapidity Z bosons collected in the Run-2. If found at the Tevatron, the q_T broadening will have a profound impact on W and Z production at the LHC.

Distinctions between the quark flavors were also neglected in the previous resummation studies, with the exception of the explicit flavor dependence in the parton densities.

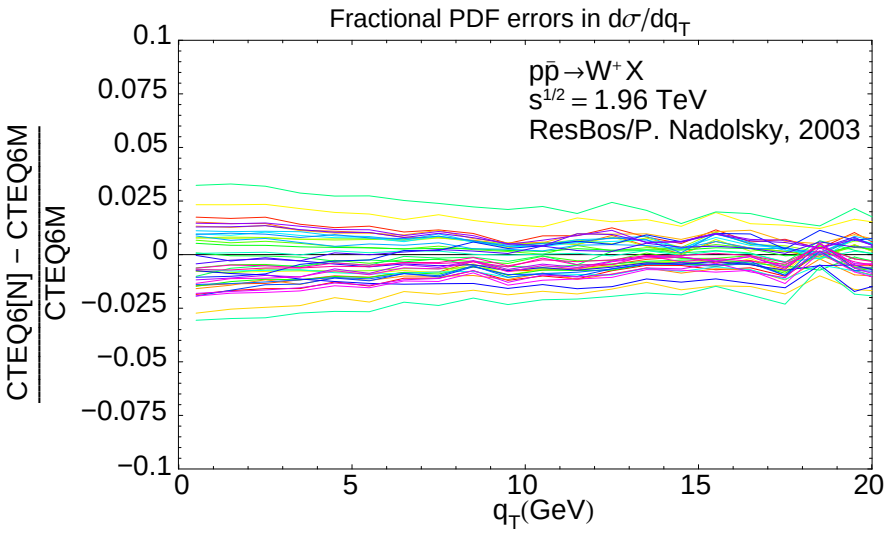

Figure 8. The PDF uncertainty in the resummed q_T distribution for W boson production in the Tevatron Run-2, evaluated using CTEQ6 PDF's [49] and BLNY form of $S_{NP}(b)$ [24]. The lines show the fractional differences between $d\sigma/dq_T$ for 40 sample PDF sets CTEQ6[N] ($N = 1, 40$), and the central PDF set (CTEQ6M).

This assumption is likely violated at some level, especially for the charm and bottom quarks, whose heavy masses suppress very soft radiation. While the heavy-quark subprocesses are rare at the Tevatron, they become important at the LHC, where about 17% (24%) of $W^+(W^-)$ bosons will be produced in scattering of charm quarks. The heavy-quark masses can be incorporated into the resummation in an extension of the CSS formalism to the massive variable-flavor number factorization scheme [37]. We estimate within this extension that the heavy-flavor mass terms will have essentially no effect on the extracted M_W in the Tevatron Run-2, but may shift M_W by ~ 5 MeV (depending on the size of the heavy-flavor nonperturbative terms) at the LHC [51].

Conclusions. The theoretical model for W and Z boson production at hadron colliders undergoes rapid development. The $\mathcal{O}(\alpha_s^2)$ QCD corrections are becoming available for many W and Z observables. The $\mathcal{O}(\alpha_s^2)$ corrections show tiny scale dependence and can be approximated in several important cases by a uniform rescaling of the $\mathcal{O}(\alpha_s)$ cross section by $2.5-5\%$. The $\mathcal{O}(\alpha_s^2)$ correction cannot be replaced by a constant K-factor when the lowest-order contribution enters at $\mathcal{O}(\alpha_s)$ (e.g., at large q_T or in leptonic angular distributions), or near the edges of phase space (e.g., at forward rapidities). The finite-order cross sections have to be improved by resummation in kinematical limits with enhanced higher-order radiation, notably at $q_T \ll Q$, but also at $q_T \gg Q$, $Q \gg M_V$, $x \to 0$, or $x \to 1$. Both formal and phenomenological aspects of the resummation formalisms require further investigation.

The $\mathcal{O}(\alpha)$ electroweak corrections are also available, and they should be applied together with the QCD corrections to reach the required accuracy. Correlations between various dynamical factors (PDF's, q_T power corrections, electroweak radiation, etc.) may be important in the full context and must be systematically explored. Finally, the newly found analytical results must be optimally implemented in numerical simulations,

which should be both fast and precise to adequately serve various practical uses.

ACKNOWLEDGMENTS

I thank my colleagues at Argonne National Laboratory, Michigan State University, and Southern Methodist University for collaboration and illuminating discussions. This work was supported in part by the US Department of Energy, High Energy Physics Division, under Contract W-31-109-ENG-38.

REFERENCES

1. M. Awramik, M. Czakon, A. Freitas, and G. Weiglein, *Phys. Rev.*, **D69**, 053006 (2004).
2. R. Brock, et al. (1999), hep-ex/0011009.
3. S. Haywood, et al. (1999), hep-ph/0003275.
4. W.-K. Tung (2004), in these proceedings, hep-ph/0410139.
5. S. Dittmaier, and M. Kramer, *Phys. Rev.*, **D65**, 073007 (2002).
6. U. Baur, O. Brein, W. Hollik, C. Schappacher, and D. Wackeroth, *Phys. Rev.*, **D65**, 033007 (2002).
7. U. Baur, S. Keller, and D. Wackeroth, *Phys. Rev.*, **D59**, 013002 (1999).
8. F. A. Berends, and R. Kleiss, *Z. Phys.*, **C27**, 365 (1985).
9. U. Baur, and D. Wackeroth (2004), hep-ph/0405191.
10. U. Baur, and T. Stelzer, *Phys. Rev.*, **D61**, 073007 (2000).
11. W. Placzek, and S. Jadach, *Eur. Phys. J.*, **C29**, 325 (2003).
12. C. M. Carloni Calame, S. Jadach, G. Montagna, O. Nicrosini, and W. Placzek, *Acta Phys. Polon.*, **B35**, 1643 (2004).
13. A. D. Martin, R. G. Roberts, W. J. Stirling, and R. S. Thorne, *Eur. Phys. J.*, **C35**, 325 (2004).
14. R. Hamberg, W. L. van Neerven, and T. Matsuura, *Nucl. Phys.*, **B359**, 343 (1991).
15. R. V. Harlander, and W. B. Kilgore, *Phys. Rev. Lett.*, **88**, 201801 (2002).
16. S. Eidelman, et al., *Phys. Lett.*, **B592**, 1 (2004).
17. P. Nadolsky, et al. (2004), in progress.
18. D. Stump, et al., *JHEP*, **10**, 046 (2003), hep-ph/0303013.
19. M. Dittmar, F. Pauss, and D. Zurcher, *Phys. Rev.*, **D56**, 7284 (1997).
20. S. Frixione, and M. L. Mangano, *JHEP*, **05**, 056 (2004).
21. C. Anastasiou, L. Dixon, K. Melnikov, and F. Petriello, *Phys. Rev.*, **D69**, 094008 (2004).
22. E. L. Berger, F. Halzen, C. S. Kim, and S. Willenbrock, *Phys. Rev.*, **D40**, 83 (1989).
23. C. Balazs, and C.-P. Yuan, *Phys. Rev.*, **D56**, 5558 (1997).
24. F. Landry, R. Brock, P. M. Nadolsky, and C.-P. Yuan, *Phys. Rev.*, **D67**, 073016 (2003).
25. W. J. Stirling, and A. D. Martin, *Phys. Lett.*, **B237**, 551 (1990).
26. J. Smith, W. L. van Neerven, and J. A. M. Vermaseren, *Phys. Rev. Lett.*, **50**, 1738 (1983).
27. S. Rajagopalan, and M. Rijssenbeek (1996), in Proc. of DPF / DPB Summer Study on New Directions in High Energy Physics (Snowmass '96).
28. W. T. Giele, and S. Keller, *Phys. Rev.*, **D57**, 4433 (1998).
29. D. Shpakov, Ph.D. thesis, Stony Brook (2000).
30. Y. L. Dokshitzer, D. Diakonov, and S. I. Troian, *Phys. Lett.*, **B79**, 269 (1978).
31. J. C. Collins, D. E. Soper, and G. Sterman, *Nucl. Phys.*, **B250**, 199 (1985).
32. J. C. Collins, and D. E. Soper, *Nucl. Phys.*, **B193**, 381 (1981), erratum: *ibid.*, **B213**, 545 (1983).
33. J. C. Collins, *Nucl. Phys.*, **B396**, 161 (1993).
34. R. Meng, F. I. Olness, and D. E. Soper, *Phys. Rev.*, **D54**, 1919 (1996).
35. P. Nadolsky, D. R. Stump, and C.-P. Yuan, *Phys. Rev.*, **D61**, 014003 (2000), erratum: *ibid.*, **D64**, 059903 (2001).
36. A. Kulesza, G. Sterman, and W. Vogelsang, *Phys. Rev.*, **D66**, 014011 (2002).
37. P. M. Nadolsky, N. Kidonakis, F. I. Olness, and C.-P. Yuan, *Phys. Rev.*, **D67**, 074015 (2003).
38. A. Weber, *Nucl. Phys.*, **B382**, 63 (1992).

39. P. M. Nadolsky, and C.-P. Yuan, *Nucl. Phys.*, **B666**, 3 (2003).
40. R. K. Ellis, and S. Veseli, *Nucl. Phys.*, **B511**, 649 (1998).
41. A. Kulesza, and W. J. Stirling, *Eur. Phys. J.*, **C20**, 349 (2001).
42. J. Qiu, and X. Zhang, *Phys. Rev.*, **D63**, 114011 (2001).
43. A. Guffanti, and G. E. Smye, *JHEP*, **10**, 025 (2000).
44. X. Ji, J.-P. Ma, and F. Yuan, *Phys. Lett.*, **B597**, 299 (2004).
45. J. C. Collins, and A. Metz (2004), hep-ph/0408249.
46. C. Anastasiou, L. J. Dixon, K. Melnikov, and F. Petriello, *Phys. Rev. Lett.*, **91**, 182002 (2003).
47. T. Affolder, et al., *Phys. Rev.*, **D64**, 052001 (2001).
48. Q.-H. Cao, and C.-P. Yuan, *Phys. Rev. Lett.*, **93**, 042001 (2004).
49. J. Pumplin, et al., *JHEP*, **07**, 012 (2002).
50. S. Berge, P. Nadolsky, F. Olness, and C. P. Yuan (2004), hep-ph/0410375.
51. S. Berge, P. Nadolsky, and F. Olness (2004), in progress.